Commun Nonlinear Sci Numer Simulat 19 (2014) 2262–2271

Contents lists available at ScienceDirect

Commun Nonlinear Sci Numer Simulat

journal homepage: www.elsevier.com/locate/cnsns

# A simple and robust boundary treatment for the forced Korteweg–de Vries equation

Hyun Geun Lee [a], Junseok Kim [b,*]

[a] Institute of Mathematical Sciences, Ewha W. University, Seoul 120-750, Republic of Korea
[b] Department of Mathematics, Korea University, Seoul 136-713, Republic of Korea

ARTICLE INFO

*Article history:*
Received 11 October 2013
Received in revised form 12 December 2013
Accepted 16 December 2013
Available online 3 January 2014

*Keywords:*
Forced Korteweg–de Vries equation
Free surface waves
Absorbing non-reflecting boundary treatment
Semi-implicit finite difference method

ABSTRACT

In this paper, we propose a simple and robust numerical method for the forced Korteweg–de Vries (fKdV) equation which models free surface waves of an incompressible and inviscid fluid flow over a bump. The fKdV equation is defined in an infinite domain. However, to solve the equation numerically we must truncate the infinite domain to a bounded domain by introducing an artificial boundary and imposing boundary conditions there. Due to unsuitable artificial boundary conditions, most wave propagation problems have numerical difficulties (e.g., the truncated computational domain must be large enough or the numerical simulation must be terminated before the wave approaches the artificial boundary for the quality of the numerical solution). To solve this boundary problem, we develop an absorbing non-reflecting boundary treatment which uses outward wave velocity. The basic idea of the proposing algorithm is that we first calculate an outward wave velocity from the solutions at the previous and present time steps and then we obtain a solution at the next time step on the artificial boundary by moving the solution at the present time step with the velocity. And then we update solutions at the next time step inside the domain using the calculated solution on the artificial boundary. Numerical experiments with various initial conditions for the KdV and fKdV equations are presented to illustrate the accuracy and efficiency of our method.



## 1. Introduction

Surface waves of an incompressible and inviscid fluid flow in a two-dimensional channel have attracted much attention. The first-order approximation of long nonlinear surface waves over a bump results in the forced Korteweg–de Vries (fKdV) equation [1–21]:

$$\eta_t + 2\lambda\eta_x - 3\eta\eta_x - (1/3)\eta_{xxx} = b_x, \quad x \in (-\infty, +\infty), \quad t > 0, \tag{1}$$

where $\eta(x,t)$ is a wave height measured from an undisturbed water level, $\lambda$ is a measurement of the perturbation of the upstream uniform flow velocity from its critical value, and $b(x)$ is a function related to the bump on the flat bottom. The fKdV equation has been used to describe many physical situations, from the flow of shallow water over rocks to atmospheric, and oceanic stratified flows encountering topographic obstacles, or even a moving pressure distribution over a free surface [22]. An important parameter in the fKdV equation is the Froude number $F = U/\sqrt{gH}$, which is defined as the ratio of the upstream velocity to the critical speed of shallow water waves, where $U$ and $H$ are the velocity and depth of the uniform

* Corresponding author. Tel.: +82 2 3290 3077; fax: +82 2 929 8562.
*E-mail address:* cfdkim@korea.ac.kr (J. Kim).
*URL:* http://math.korea.ac.kr/~cfdkim (J. Kim).

1007-5704/$ - see front matter © 2013 Elsevier B.V. All rights reserved.
http://dx.doi.org/10.1016/j.cnsns.2013.12.019

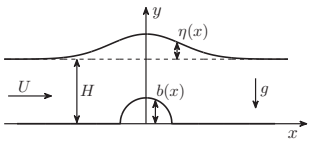


**Fig. 1.** Configuration of the flow forced by a bump on the flat bottom of a two-dimensional channel.

flow far upstream, respectively, and $g$ is the gravitational acceleration (see Fig. 1). $F = 1 + \epsilon\lambda$ and $\epsilon$ is a small positive number. If $F > 1$ ($F < 1$), the flow is called supercritical (subcritical). If $F > 1$ on one side and $F < 1$ on the other side, the flow is called critical. The terms critical, subcritical, and supercritical come from linear theory [23].

In the absence of a forcing term $b_x$, the KdV equation is completely integrable and its solitary wave solutions can be found analytically [24–32], while the fKdV equation is not known to be integrable and thus is studied mainly numerically. Forbes and Schwartz [1] used the boundary integral method to obtain numerical solutions of the two-dimensional steady flow of a fluid over a semi-circular obstacle. Vanden–Broeck [3] discovered the existence of two branches of supercritical positive solitary wave solutions of the stationary fKdV equation. Forbes [4] computed numerical solutions of critical flow over a semi-circular obstacle using the formulation of Forbes and Schwartz [1]. The flow was a uniform subcritical stream ahead of the obstacle, followed by a uniform supercritical stream behind the obstacle. This type of solution is generally referred to as 'hydraulic fall'. Camassa and Wu [5,6] performed a stability analysis of forced steady solitary-wave solutions when the forcing term is given as a $\mathrm{sech}^4(x)$-profile, and confirmed their analytical findings with accurate numerical simulations. Gong and Shen [7] studied supercritical positive solitary wave solutions of the stationary fKdV equation under three types of forcing functions, including a well-shape forcing, a sine-shape forcing, and a two semi-elliptic bump forcing. Shen et al. [12] demonstrated numerically the collision process of the solitary waves in the fKdV equation using a semi-implicit pseudo-spectral method. In the case of a single obstacle, Dias and Vanden–Broeck [13] found new solutions called 'generalized hydraulic falls'. These solutions are characterized by a supercritical flow on one side of the obstacle and a train of waves on the other. Dias and Vanden–Broeck [14] computed new solutions for the flow past two obstacles of arbitrary shape. These solutions are characterized by a train of waves 'trapped' between the obstacles. Choi et al. [18] studied solutions of the fKdV equation with zero and nonzero initial conditions using a generalized Crank–Nicolson scheme for the time discretization and a Fourier-spectral method for the space discretization. Donahue and Shen [19] demonstrated numerically the stability of the hydraulic fall and cnoidal wave solution of the fKdV equation using a semi-implicit spectral method. Chardard et al. [20] derived solutions of the stationary fKdV equation and studied their stability analytically and numerically.

The KdV and fKdV equations are originally defined in an infinite domain. When numerical simulations of the KdV and fKdV equations are performed, it is a common practice to truncate the infinite domain to a bounded domain by introducing an artificial boundary and imposing boundary conditions there. A proper choice of these boundary conditions should mimic the absorption of waves traveling through the artificial boundary to the exterior domain and makes the truncated problem equivalent to the full system. However, a poor choice of artificial boundary conditions may change the qualitative behavior of the solutions due to spurious wave reflection [33]. In many previous studies for nonlinear waves [7,11,12,16,18–21,34–42], periodic boundary conditions and zero Dirichlet boundary conditions were mainly used. Due to unsuitable artificial boundary conditions, the truncated problem has numerical difficulties such as large computational domain and early termination of the computation. To overcome these difficulties, we develop an absorbing non-reflecting boundary treatment which uses outward wave velocity. We first calculate an outward wave velocity at the domain boundary from the solutions of previous time steps and then we obtain a solution at the next time step on the artificial boundary. And we next update solutions at the next time step inside the domain using the calculated solution on the artificial boundary.

The paper is organized as follows. In Section 2, we present a simple and robust boundary treatment for the fKdV equation. We perform some characteristic numerical experiments with various initial conditions for the KdV and fKdV equations to illustrate the accuracy and efficiency of our method in Section 3. Finally, conclusions are drawn in Section 4.

## 2. Numerical solution

In this section, we describe a simple and robust boundary treatment for the fKdV equation on a bounded domain. Let $\Omega = [\alpha, \beta]$ be a bounded computational domain which contains the compact support of $b(x)$, $N_x$ be a positive integer, $h = (\beta - \alpha)/N_x$ be a grid size, and $x_i = \alpha + (i-1)h$ for $i = 1, \ldots, N_x + 1$. Let $\eta_i^n$ be an approximation of $\eta(x_i, n\Delta t)$ for $n = 0, \ldots, N_t$, where $\Delta t = T/N_t$ is a time step size, $T$ is a final time, and $N_t$ is a total number of time steps.

A fully implicit discretization of Eq. (1) takes the form

$$\frac{\eta_i^{n+1} - \eta_i^n}{\Delta t} + \left(2\lambda - 3\eta_i^{n+1}\right)\frac{\eta_{i+1}^{n+1} - \eta_{i-1}^{n+1}}{2h} - \frac{\eta_{i+2}^{n+1} - 2\eta_{i+1}^{n+1} + 2\eta_{i-1}^{n+1} - \eta_{i-2}^{n+1}}{6h^3} = \frac{b_{i+1} - b_{i-1}}{2h}. \tag{2}$$

Eq. (2) is nonlinear in terms of the unknown variable $\eta_i^{n+1}$. To avoid this, we approximate the nonlinear term $\eta_i^{n+1}\frac{\eta_{i+1}^{n+1} - \eta_{i-1}^{n+1}}{2h}$ by $\eta_i^{n+\frac{1}{2}}\frac{\eta_{i+1}^{n+1} - \eta_{i-1}^{n+1}}{2h}$, where the half time value $\eta_i^{n+\frac{1}{2}}$ is calculated using an extrapolation from previous values, i.e., $\eta_i^{n+\frac{1}{2}} = 2\eta_i^n - \eta_i^{n-1}$. This yields

$$\frac{\eta_i^{n+1}-\eta_i^n}{\Delta t}+\left(2\lambda-3\eta_i^{n+\frac{1}{2}}\right)\frac{\eta_{i+1}^{n+1}-\eta_{i-1}^{n+1}}{2h}-\frac{\eta_{i+2}^{n+1}-2\eta_{i+1}^{n+1}+2\eta_{i-1}^{n+1}-\eta_{i-2}^{n+1}}{6h^3}=\frac{b_{i+1}-b_{i-1}}{2h}. \tag{3}$$

Eq. (3) can be rearranged as

$$\frac{1}{6h^3}\eta_{i-2}^{n+1}-\left(\frac{2\lambda-3\eta_i^{n+\frac{1}{2}}}{2h}+\frac{1}{3h^3}\right)\eta_{i-1}^{n+1}+\frac{1}{\Delta t}\eta_i^{n+1}+\left(\frac{2\lambda-3\eta_i^{n+\frac{1}{2}}}{2h}+\frac{1}{3h^3}\right)\eta_{i+1}^{n+1}-\frac{1}{6h^3}\eta_{i+2}^{n+1}=\frac{1}{\Delta t}\eta_i^n+\frac{b_{i+1}-b_{i-1}}{2h}. \tag{4}$$

The advantages of this semi-implicit discretization are (i) the resulting difference equation is linear in $\eta_i^{n+1}$ and (ii) the linear system formed in Eq. (4) is a pentadiagonal matrix which can be inverted directly [43]. Note that a two-step method needs two values $\eta_i^{-1}$ and $\eta_i^0$ in order to start the time integration (4). From the given initial condition $\eta_i^0$, we set $\eta_i^{-1}=\eta_i^0$ for convenience.

Since we truncate the unbounded domain to a bounded domain by introducing artificial boundaries, nonreflecting boundary conditions are needed to ensure that no (or little) spurious wave reflection occurs from the artificial boundaries. Naturally, the quality of the numerical solution depends on the boundary conditions. We propose a new simple and robust boundary treatment which is based on the fact that the solution of the equation

$$\eta_t+c\eta_{xxx}=0 \tag{5}$$

propagates in the opposite direction to the sign of a constant $c$. We consider the Fourier mode

$$\eta(x,t)=\hat{\eta}e^{i(\gamma x+\omega t)}, \tag{6}$$

where $\omega$ is the frequency and $\gamma$ is the wave number. If we insert Eq. (6) into Eq. (5), the dispersion relation for Eq. (5) is $\omega=\gamma^3 c$.Therefore, the wave propagates with speed $-\omega/\gamma=-\gamma^2 c$ [44]. For example, the time evolution of the solution of $\eta_t-\eta_{xxx}=0$ is shown in Fig. 2 for the following initial conditions: $\eta(x,0)=\sin(x)$ and $\eta(x,0)=\sin(2x)$. Note that the wave number of the second initial condition is twice that of the first initial condition. Clearly, the solutions associated with different wave numbers propagate with different velocities (the solution corresponding to the second initial condition moves four times faster than that corresponding to the first initial condition). From the fact that the solution moves with a velocity (see Fig. 2), we can approximate the solution at the $(n+1)$th time step by the solution at the $n$th time step and velocity.

In the fKdV equation (1), solitary waves are generated at the bump and propagate to the boundaries. Therefore, in our method, for each time step we calculate the outward wave velocities from the solutions at time steps $n$ and $n-1$. Using these velocities, we extrapolate the solutions $(\eta_0^{n+1},\eta_1^{n+1},\eta_{N_x+1}^{n+1}$, and $\eta_{N_x+2}^{n+1})$ at the $(n+1)$th time step near or on artificial boundaries from the solutions at time steps $n$ and $n-1$. Then, we calculate the solutions $(\eta_2^{n+1},\ldots,\eta_{N_x}^{n+1})$ at the $(n+1)$th time step in the interior region with the extrapolated solutions.

Let us now describe an algorithm for approximating $\eta_0^{n+1}$, $\eta_1^{n+1}$, $\eta_{N_x+1}^{n+1}$, and $\eta_{N_x+2}^{n+1}$. Since the treatment of the two boundaries is essentially identical, we consider only the right boundary. To find $\eta_{N_x+1}^{n+1}$ and $\eta_{N_x+2}^{n+1}$, we follow the procedure below.

Step 1. Given three points $(x_{N_x-1},\eta_{N_x-1}^n)$, $(x_{N_x},\eta_{N_x}^n)$, and $(x_{N_x+1},\eta_{N_x+1}^n)$ on the wave (see Fig. 3), we find a quadratic function $f(x)=ax^2+bx+c$ which passes through the three points:

$$\begin{pmatrix}a\\b\\c\end{pmatrix}=\begin{pmatrix}x_{N_x-1}^2 & x_{N_x-1} & 1\\ x_{N_x}^2 & x_{N_x} & 1\\ x_{N_x+1}^2 & x_{N_x+1} & 1\end{pmatrix}^{-1}\begin{pmatrix}\eta_{N_x-1}^n\\ \eta_{N_x}^n\\ \eta_{N_x+1}^n\end{pmatrix}.$$

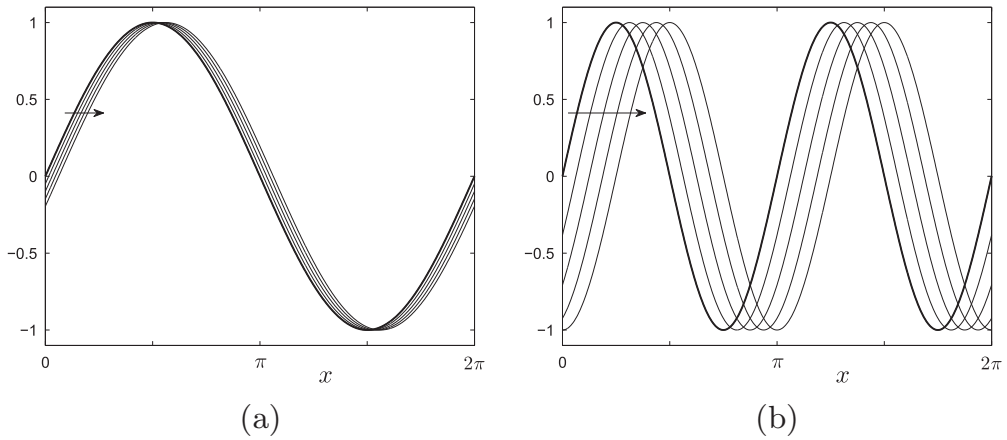


**Fig. 2.** Time evolution of the solution of $\eta_t-\eta_{xxx}=0$ for two initial conditions: (a) $\eta(x,0)=\sin(x)$ and (b) $\eta(x,0)=\sin(2x)$. In each figure, times are $t=0,\ \pi/64,\pi/48,\pi/32$, and $\pi/16$ (from left to right). The wave in (b) moves four times faster than that in (a).

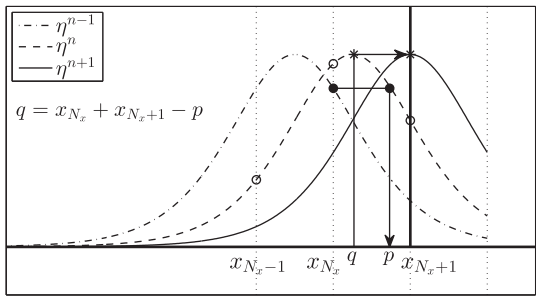


**Fig. 3.** Schematic diagram for finding $\eta^{n+1}_{N_x+1}$ (star symbol).

Step 2. Using the bisection algorithm [45], we find a solution $p$ to $f(x) = \eta^{n-1}_{N_x}$ on the interval $[x_{N_x}, x_{N_x+1}]$.
Step 3. We take $\eta^{n+1}_{N_x+1}$ as $f(x_{N_x} + x_{N_x+1} - p)$. The boundary value $\eta^{n+1}_{N_x+2}$ is computed in a similar manner.

Owing to the proposed boundary treatment, we can simulate the absorption of waves traveling through the artificial boundaries to the exterior domain. Therefore, in contrast to previous studies, it is possible to run the numerical simulation on the small computational domain until and after the waves reach the artificial boundary.

## 3. Numerical experiments

In this section, we perform some characteristic numerical experiments with various initial conditions for the KdV and fKdV equations to illustrate the accuracy and efficiency of our method. We define the error of the numerical solution as [46]

$$e^n_{\max} = \max_i |\eta^n_i - \eta(x_i, n\Delta t)|.$$

Unless otherwise specified, the forcing term $b(x)$ in Eq. (1) is chosen as $b(x) = \sqrt{1-x^2}$ for $|x| \leqslant 1$ and $b(x) = 0$ for $|x| > 1$, and we take the time and space step sizes as $10^{-4}$ and $10^{-2}$, respectively.

### 3.1. Traveling wave solutions

For $c < 2\lambda$, the KdV equation, $\eta_t + 2\lambda\eta_x - 3\eta\eta_x - (1/3)\eta_{xxx} = 0$, has a traveling solitary-wave solution

$$S_{c,x_0}(x,t) = (2\lambda - c)\mathrm{sech}^2\left(\sqrt{3(2\lambda - c)}(x - x_0 - ct)/2\right),$$

where $c$ stands for the traveling velocity of the wave and $x_0$ is a phase shift. With $c > 0$, the traveling solitary wave moves to the downstream. Thus, in previous studies, the numerical simulation was terminated before the wave reaches artificial boundary due to wave reflection. To examine the performance of our method, we consider the following initial condition:

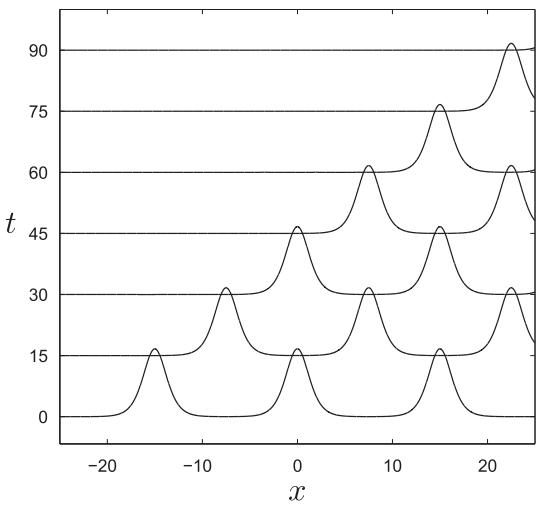


**Fig. 4.** Time evolution of the solution $\eta$ of $\eta_t + 2\lambda\eta_x - 3\eta\eta_x - (1/3)\eta_{xxx} = 0$ with $\lambda = 0.5$ and $c = 0.5$.

$$\eta(x,0) = S_{c,x_0}(x,0) + S_{c,x_1}(x,0) + S_{c,x_2}(x,0)$$

on the domain $\Omega = [-25, 25]$ with $\lambda = 0.5,\ c = 0.5,\ x_0 = -15,\ x_1 = 0$, and $x_2 = 15$. Fig. 4 shows the time evolution of the solution $\eta$ of the KdV equation. It is clear that the simulation continues until the waves completely move out of the domain due to our boundary treatment.

### 3.2. Single and two soliton solutions – comparison with previous results

In [35], the following KdV equation,

$$\eta_t + 6\eta\eta_x + \eta_{xxx} = 0, \tag{7}$$

is studied numerically by the semi-implicit method and zero Dirichlet boundary conditions. A single soliton solution of Eq. (7) is

$$\eta(x,t) = \frac{c}{2}\operatorname{sech}^2\left(\frac{\sqrt{c}}{2}(x - ct + x_0)\right),$$

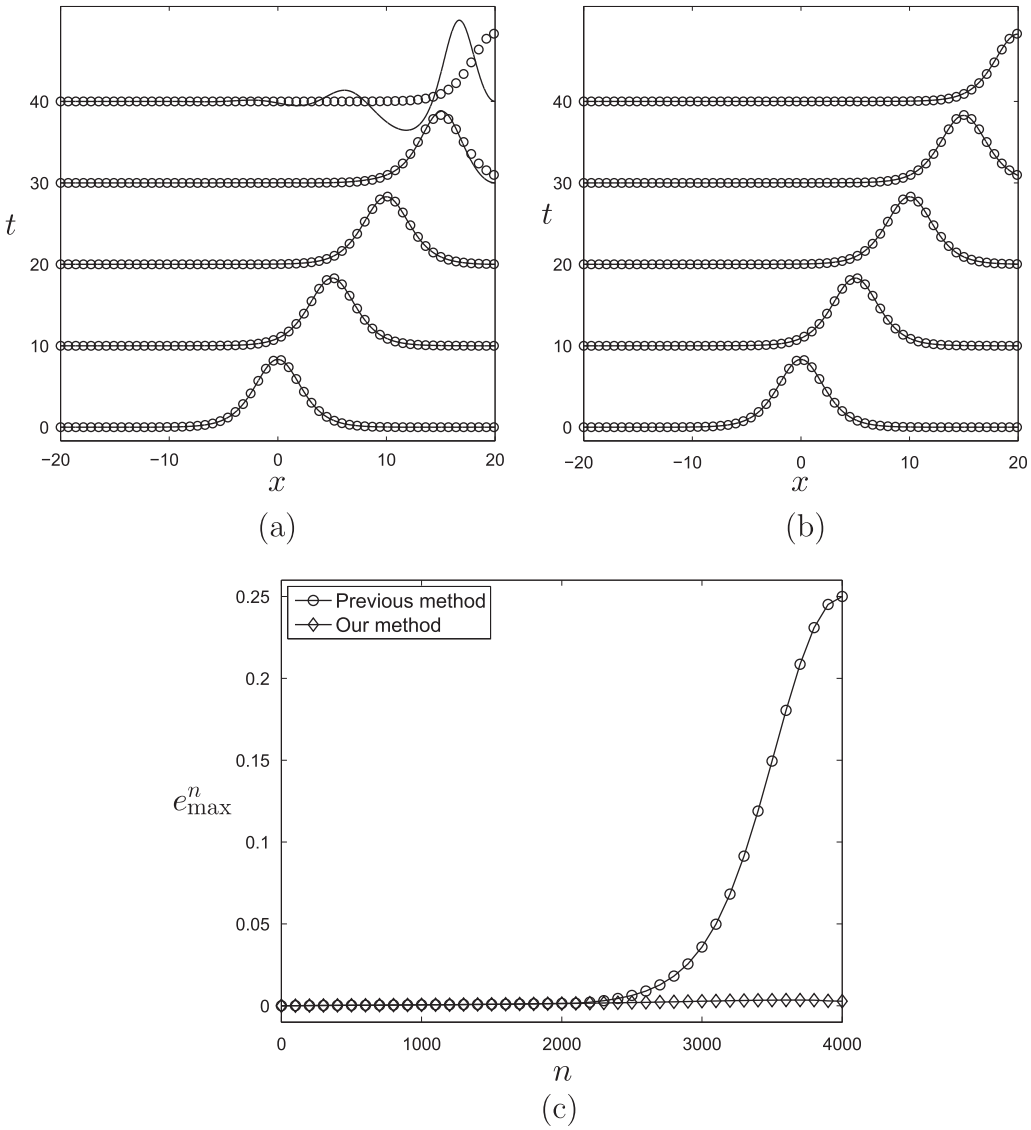


**Fig. 5.** Time evolution of the single soliton solution $\eta$ of $\eta_t + 6\eta\eta_x + \eta_{xxx} = 0$ obtained with the boundary treatment in Ref. [35] (a) and in our method (b). Solid lines and open circles represent the numerical and exact solutions, respectively. For both, we take $h = 10^{-2}$ and $\Delta t = 10^{-2}$. (c) Evolution of the error $e^n_{\max}$ with iteration number for both methods. The errors $e^n_{\max}$ at $t = 40$ are 2.50e−1 and 2.80e−3 for previous and our methods, respectively.

where $x_0$ is the initial position of the soliton and $c$ is related to the amplitude of the soliton. For the initial wave $\eta(x,0)=\frac{1}{4}\mathrm{sech}^2\left(\frac{\sqrt{0.5}}{2}x\right)$ on the domain $\Omega=[-20,20]$, Fig. 5(a) and (b) show the time evolution of the solution $\eta$ of Eq. (7) obtained with the boundary treatment in Ref. [35] and in our method, respectively. And the evolution of the error $e^n_{\max}$ with iteration number for both methods is shown in Fig. 5(c). For both, we take $h=10^{-2}$ and $\Delta t=10^{-2}$. From $t=0$ until $t=20$, the numerical results of both cases stay very close to the exact solutions (the errors $e^n_{\max}$ at $n=2000$ ($t=20$) are 1.43e−3 and 1.35e−3 for previous and our methods, respectively). However, in the former case (Fig. 5(a)), as time evolves, i.e., as the wave approaches the artificial boundary, the large error comes from the artificial boundary (the errors $e^n_{\max}$ at $t=30$ and 40 are 3.58e−2 and 2.50e−1, respectively). In the latter case (Fig. 5(b)), the error $e^n_{\max}$ is less than 3.49e−3 during our entire simulation.

Next, a particular case with the initial condition $\eta(x,0)=6\mathrm{sech}^2 x$ yields a two soliton solution

$$\eta(x,t)=12\frac{3+4\cosh(2x-8t)+\cosh(4x-64t)}{[3\cosh(x-28t)+\cosh(3x-36t)]^2}.$$

Note that the initial wave disintegrates into two solitons as time evolves. We take the initial condition as $\eta(x,0)=6\mathrm{sech}^2 x$ on the domain $\Omega=[-10,10]$, and use $h=10^{-2}$ and $\Delta t=10^{-5}$. Fig. 6(a) and (b) show the time evolution of the solution $\eta$ of Eq. (7) obtained with the boundary treatment in Ref. [35] and in our method, respectively. And the evolution of the error $e^n_{\max}$ with iteration number for both methods is shown in Fig. 6(c). For both, the error $e^n_{\max}$ is less than 1.24e−1 within $t=0.5$.

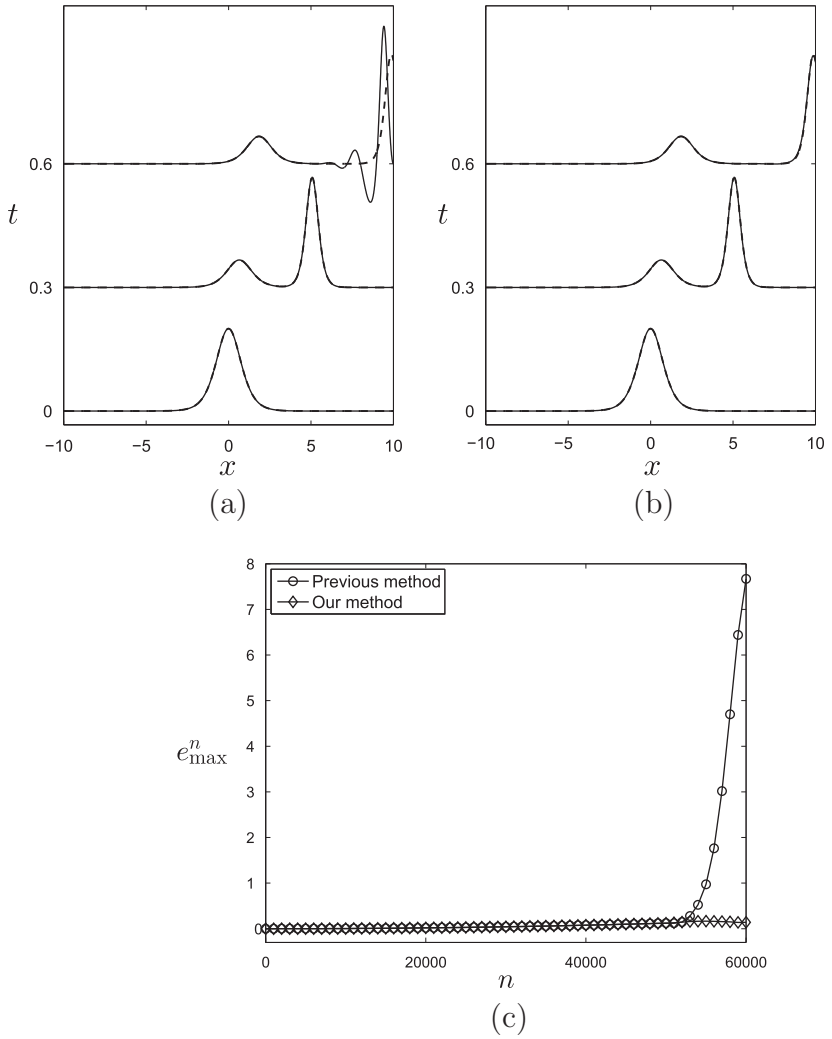


**Fig. 6.** Time evolution of the two soliton solution $\eta$ of $\eta_t+6\eta\eta_x+\eta_{xxx}=0$ obtained with the boundary treatment in Ref. [35] (a) and in our method (b). Solid and dashed lines represent the numerical and exact solutions, respectively. For both, we take $h=10^{-2}$ and $\Delta t=10^{-5}$. (c) Evolution of the error $e^n_{\max}$ with iteration number for both methods. The errors $e^n_{\max}$ at $t=0.6$ are 7.66 and 1.39e−1 for previous and our methods, respectively.

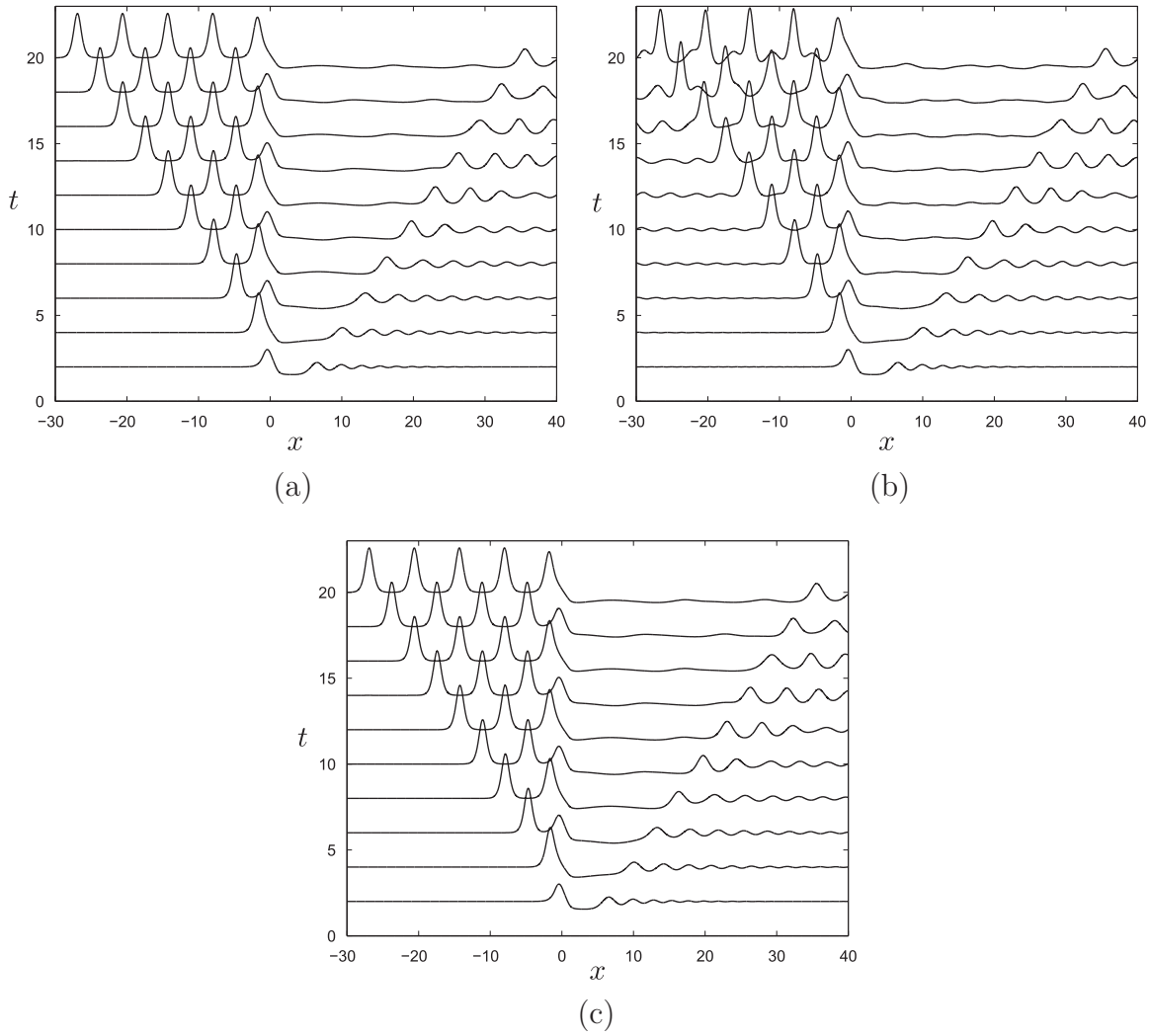


**Fig. 7.** Time evolution of the solution $\eta$ of the fKdV equation with zero initial condition. (a) Results obtained by the spectral method for $\Omega = [-600, 600]$ (the figure is shown only for $-30 \leqslant x \leqslant 40$). (b) Results obtained by the spectral method for $\Omega = [-30, 40]$. (c) Results obtained by our method for $\Omega = [-30, 40]$.

However, when $t = 0.6$, the error $e^n_{\max}$ of the former case is 7.66 while the error $e^n_{\max}$ of the latter case is 1.39e−1. As we can see in Figs. 5 and 6, our method can produce permeable and non-reflecting waves in a small bounded domain.

### *3.3. Numerical solutions with zero initial condition – comparison with previous results*

In this section, numerical solutions of the fKdV Eq. (1) with zero initial condition $\eta(x, 0) \equiv 0$ are discussed. In previous studies used the spectral method, the sufficiently large computational domain was employed to satisfy the periodicity required by the spectral method used. Fig. 7(a) shows the time evolution of the solution $\eta$ of Eq. (1) using the spectral method. In this simulation, a generalized Crank–Nicolson scheme is used to discretize the temporal variable, the periodic boundary conditions are used for the spatial variable, and the computational domain is $\Omega = [-600, 600]$ (this problem setting is the same as Section 4.3.2 of Ref. [18]). Owing to the sufficiently large computational domain, there is no spurious wave reflection occurs from artificial boundaries. However, when the computational domain is small ($\Omega = [-30, 40]$ in Fig. 7(b)), small oscillatory waves are generated and the stem waves are broken. Fig. 7(c) shows the time evolution of the solution $\eta$ on $\Omega = [-30, 40]$ using our method. As we can see, the results in Fig. 7(c) are qualitatively in agreement with the results in Fig. 7(a) despite the use of small computational domain. Owing to the use of small computational domain, the CPU time used in our method (241.1 s) is less than the one needed in the spectral method (2565.3 s).

As we can see in Fig. 7, our method does not have a domain size dependency. To investigate the domain size dependency in more detail, we perform a number of simulations for the above problem on $\Omega = [-30, 40], [-30, 50]$, and $[-30, 60]$. Fig. 8 shows the time evolution of the solution $\eta$ on $\Omega = [-30, 40]$ (open circles), $[-30, 50]$ (stars), and $[-30, 60]$ (diamonds). Since

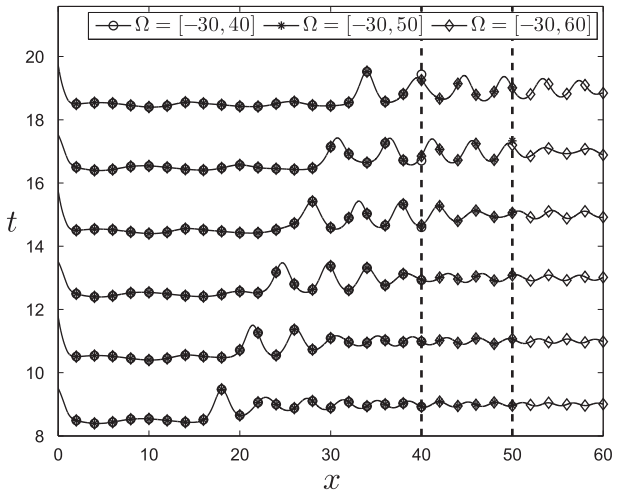


**Fig. 8.** Time evolution of the solution $\eta$ on $\Omega = [-30, 40]$ (open circles), $[-30, 50]$ (stars), and $[-30, 60]$ (diamonds). Times are $t = 10$, 12, 14, 16, 18, and 20 (from bottom to top). Our method does not have a domain size dependency.

our method does not produce reflecting waves, we can obtain qualitatively the same solutions near and on the artificial boundaries regardless of domain size.

Next, in Fig. 7(a), there is no spurious wave reflection in the short time simulation since the waves generated by the bump do not yet reach the boundary of the sufficiently large computational domain. To investigate the long time behavior of the solution $\eta$, we run the simulation for the problem in Fig. 7(a) until $t = 200$. Figs. 9(a) and (b) show the solution $\eta$ on $\Omega = [-600, 600]$ obtained by the spectral and proposed methods at $t = 200$, respectively. In the case of the spectral method (Fig. 9(a)), as time evolves, the waves, which propagate to the right boundary and then move out, reenter through the left boundary due to the periodicity. As a result, in the long time simulation, there are oscillatory waves with high amplitude despite the use of sufficiently large computational domain (see the left part of Fig. 9(a)). However, in the case of the proposed method (Fig. 9(b)), there is still no spurious wave reflection and no oscillatory wave in the long time simulation.

### 3.4. Evolution of the error on the boundary

To illustrate the capability of our method for absorbing the waves without reflection, we solve the fKdV equation (1) with zero initial condition $\eta(x, 0) \equiv 0$ on $\Omega = [-40, 40]$. Note that we consider a reference solution $\eta^n_{\text{ref}}$, because it is generally hard to find the exact solution of the fKdV equation. We define the reference solution $\eta^n_{\text{ref}}$ as the numerical solution calculated on $\Omega = [-600, 600]$ with zero Dirichlet boundary conditions, $\eta(x, t) = 0$ at $x = -600$, 600 (we employ the sufficiently large com-

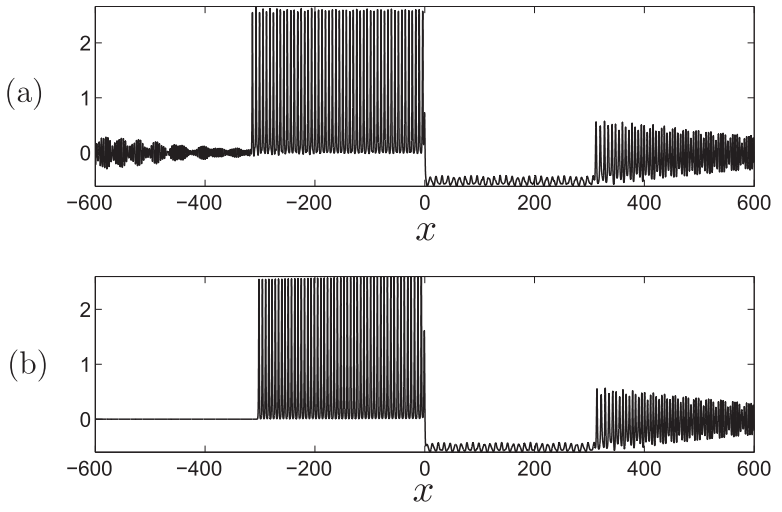


**Fig. 9.** Long time simulation of the solution $\eta$ on $\Omega = [-600, 600]$. (a) and (b) are the results obtained by the spectral and proposed methods at $t = 200$, respectively.

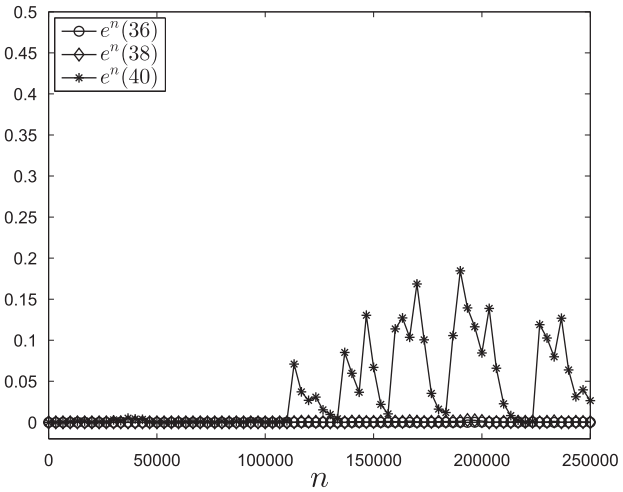


**Fig. 10.** Evolution of the error $e^n(x) = |\eta^n(x) - \eta^n_{\text{ref}}(x)|$ at $x = 36, 38, 40$ with iteration number.

putational domain to avoid the wave reflection occurs from artificial boundaries due to the boundary conditions) and then define the error as $e^n(x) = |\eta^n(x) - \eta^n_{\text{ref}}(x)|$. Fig. 10 shows the evolution of the error $e^n(x)$ at $x = 36, 38, 40$ with iteration number. At $x = 40$, the errors on a short time scale are zero or very small, but the errors on a long time scale are large compared to those on a short time scale. However, our method allows to absorb the waves, which travel through the artificial boundary to the exterior domain, without reflection, and as a result, the errors at $x = 36, 38$ are zero or very small on both short and long time scales, i.e., the interior waves are almost not affected by the artificial boundary.

## 4. Conclusions

In this paper, we proposed a simple and robust numerical method for the fKdV equation. To solve the fKdV equation numerically we must truncate an infinite domain to a finite domain by introducing an artificial boundary and imposing boundary conditions there. Due to unsuitable artificial boundary conditions, most wave propagation problems have numerical difficulties. To solve this boundary problem, we developed an absorbing non-reflecting boundary treatment which uses outward wave velocity. The basic idea of the technique was that we first calculate an outward wave velocity from the solutions at the previous and present time steps and then we obtain a solution at the next time step on the artificial boundary by moving the solution at the present time step with the velocity. And we next update solutions at the next time step inside the domain using the calculated solution on the artificial boundary. Numerical experiments with various initial conditions for the KdV and fKdV equations were presented to illustrate the accuracy and efficiency of our method. Owing to our boundary treatment, we could simulate the absorption of waves traveling through the artificial boundary to the exterior domain without reflection. Therefore, in contrast to previous studies, it was possible to run the numerical simulation on the small computational domain until and after the waves reach the artificial boundary.

## Acknowledgment

The first author (Hyun Geun Lee) was supported by Basic Science Research Program through the National Research Foundation of Korea (NRF) funded by the Ministry of Education (2009-0093827). The authors thank the reviewers for the constructive and helpful comments on the revision of this article. The corresponding author (J.S. Kim) also thanks Professor Jeong-Whan Choi for suggesting this problem and for valuable discussions.

## References

[1] Forbes LK, Schwartz LW. Free-surface flow over a semicircular obstruction. J Fluid Mech 1982;114:299–314.
[2] Miles JW. Stationary, transcritical channel flow. J Fluid Mech 1986;162:489–99.
[3] Vanden-Broeck J-M. Free-surface flow over an obstruction in a channel. Phys Fluids 1987;30:2315–7.
[4] Forbes LK. Critical free-surface flow over a semi-circular obstruction. J Eng Math 1988;22:3–13.
[5] Camassa R, Yao-Tsu Wu T. Stability of forced steady solitary waves. Philos Trans R Soc Lond A 1991;337:429–66.
[6] Camassa R, Yao-Tsu Wu T. Stability of some stationary solutions for the forced KdV equation. Physica D 1991;51:295–307.
[7] Gong L, Shen SS. Multiple supercritical solitary wave solutions of the stationary forced Korteweg–de Vries equation and their stability. SIAM J Appl Math 1994;54:1268–90.
[8] Shen SS-P. On the accuracy of the stationary forced Korteweg–de Vries equation as a model equation for flows over a bump. Q Appl Math 1995;53:701–19.
[9] Shen SS, Manohar RP, Gong L. Stability of the lower cusped solitary waves. Phys Fluids 1995;7:2507–9.

[10] Choi JW, Sun SM, Shen MC. Internal capillary-gravity waves of a two-layer fluid with free surface over an obstruction – forced extended KdV equation. Phys Fluids 1996;8:397–404.
[11] Milewski PA, Vanden-Broeck J-M. Time dependent gravity-capillary flows past an obstacle. Wave Motion 1999;29:63–79.
[12] Shen SSP, Shen B, Ong CT, Xu ZT. Collision of uniform soliton trains in asymmetric systems. Dyn Contin Dis Ser B 2002;9:131–8.
[13] Dias F, Vanden-Broeck J-M. Generalised critical free-surface flows. J Eng Math 2002;42:291–301.
[14] Dias F, Vanden-Broeck J-M. Trapped waves between submerged obstacles. J Fluid Mech 2004;509:93–102.
[15] Dias F, Vanden-Broeck J-M. Two-layer hydraulic falls over an obstacle. Eur J Mech B Fluids 2004;23:879–98.
[16] Cabral M, Rosa R. Chaos for a damped and forced KdV equation. Physica D 2004;192:265–78.
[17] Binder BJ, Vanden-Broeck J-M, Dias F. Forced solitary waves and fronts past submerged obstacles. Chaos 2005;15:037106-1–037106–13.
[18] Choi JW, Sun SM, Whang SI. Supercritical surface gravity waves generated by a positive forcing. Eur J Mech B Fluids 2008;27:750–70.
[19] Donahue AS, Shen SSP. Stability of hydraulic fall and sub-critical cnoidal waves in water flows over a bump. J Eng Math 2010;68:197–205.
[20] Chardard F, Dias F, Nguyen HY, Vanden-Broeck J-M. Stability of some stationary solutions to the forced KdV equation with one or two bumps. J Eng Math 2011;70:175–89.
[21] Kim H, Bae W-S, Choi J. Numerical stability of symmetric solitary-wave-like waves of a two-layer fluid – forced modified KdV equation. Math Comput Simul 2012;82:1219–27.
[22] Baines PG. Topographic effects in stratified flows. New York: Cambridge University Press; 1995.
[23] Zhang Y, Zhu S. Subcritical, transcritical and supercritical flows over a step. J Fluid Mech 1997;333:257–71.
[24] Hirota R. Exact solution of the Korteweg–de Vries equation for multiple collisions of solitons. Phys Rev Lett 1971;27:1192–4.
[25] Yan C. A simple transformation for nonlinear waves. Phys Lett A 1996;224:77–84.
[26] Wazwaz A-M. The tanh method for traveling wave solutions of nonlinear equations. Appl Math Comput 2004;154:713–23.
[27] Wazwaz A-M. New sets of solitary wave solutions to the KdV, mKdV, and the generalized KdV equations. Commun Nonlinear Sci Numer Simul 2008;13:331–9.
[28] Lu D, Hong B, Tian L. New solitary wave and periodic wave solutions for general types of KdV and KdV–Burgers equations. Commun Nonlinear Sci Numer Simul 2009;14:77–84.
[29] Wazzan L. A modified tanh–coth method for solving the KdV and the KdV–Burgers' equations. Commun Nonlinear Sci Numer Simul 2009;14:443–50.
[30] Kudryashov NA. On new travelling wave solutions of the KdV and the KdV–Burgers equations. Commun Nonlinear Sci Numer Simul 2009;14:1891–900.
[31] Kudryashov NA. Meromorphic solutions of nonlinear ordinary differential equations. Commun Nonlinear Sci Numer Simul 2010;15:2778–90.
[32] Triki H, Wazwaz A-M. Traveling wave solutions for fifth-order KdV type equations with time-dependent coefficients. Commun Nonlinear Sci Numer Simul 2014;19:404–8.
[33] Carpio A, Tapiador B. Nonreflecting boundary conditions for discrete waves. J. Comput. Phys. 2010;229:1879–96.
[34] Shamardan AB. Central finite difference schemes for nonlinear dispersive waves. Comput Math Appl 1990;19:9–15.
[35] Li P-W. On the numerical study of the KdV equation by the semi-implicit and Leap-frog method. Comput Phys Commun 1995;88:121–7.
[36] Jain PC, Shankar R, Bhardwaj D. Numerical solution of the Korteweg–de Vries (KdV) equation. Chaos Soliton Fract 1997;8:943–51.
[37] Ismail MS. Numerical solution of complex modified Korteweg–de Vries equation by collocation method. Commun Nonlinear Sci Numer Simul 2009;14:749–59.
[38] Zhang J, Yan G. A lattice Boltzmann model for the Korteweg–de Vries equation with two conservation laws. Comput Phys Commun 2009;180:1054–62.
[39] Korkmaz A, Dağ İ. Solitary wave simulations of complex modified Korteweg–de Vries equation using differential quadrature method. Comput Phys Commun 2009;180:1516–23.
[40] Bai D, Zhang L. Numerical studies on a novel split-step quadratic B-spline finite element method for the coupled Schrodinger–KdV equations. Commun Nonlinear Sci Numer Simul 2011;16:1263–73.
[41] Kudryashov NA, Ryabov PN, Sinelshchikov DI. Nonlinear waves in media with fifth order dispersion. Phys Lett A 2011;375:2051–5.
[42] Wang M, Li D, Zhang C, Tang Y. Long time behavior of solutions of gKdV equations. J Math Anal Appl 2012;390:136–50.
[43] Cheney W, Kincaid D. Numerical mathematics and computing. Boston: Brooks/Cole; 2013.
[44] Thomas JW. Numerical partial differential equations: finite difference methods. New York: Springer; 1995.
[45] Burden RL, Faires JD. Numerical analysis. Boston: Brooks/Cole; 2011.
[46] Kudryashov NA, Ryabov PN, Fedyanin TE, Kutukov AA. Evolution of pattern formation under ion bombardment of substrate. Phys Lett A 2013;377:753–9.